The Role of SLIT3–ROBO4 Signaling in Endoplasmic Reticulum Stress–Induced Delayed Corneal Epithelial and Nerve Regeneration

Rong Chen,[1] Yao Wang,[1] Zhenzhen Zhang,[1] Xiaolei Wang,[1] Ya Li,[1] Min Wang,[1] Huifeng Wang,[1] Muchen Dong,[2] Qingjun Zhou,[1] and Lingling Yang[1]

[1]State Key Laboratory Cultivation Base, Shandong Provincial Key Laboratory of Ophthalmology, Shandong Eye Institute, Shandong First Medical University & Shandong Academy of Medical Sciences, Qingdao, China
[2]Eye Institute of Shandong First Medical University, Eye Hospital of Shandong First Medical University (Shandong Eye Hospital), Jinan, China

Correspondence: Lingling Yang, State Key Laboratory Cultivation Base, Shandong Provincial Key Laboratory of Ophthalmology, Shandong Eye Institute, Shandong First Medical University & Shandong Academy of Medical Sciences, 5 Yan'er dao Road, Qingdao 266071, China;
lingling6008@126.com.

Received: November 3, 2023
Accepted: March 23, 2024
Published: May 3, 2024

Citation: Chen R, Wang Y, Zhang Z, et al. The role of SLIT3–ROBO4 signaling in endoplasmic reticulum stress–induced delayed corneal epithelial and nerve regeneration. *Invest Ophthalmol Vis Sci.* 2024;65(5):8.
https://doi.org/10.1167/iovs.65.5.8

Purpose. In the present study, we aim to elucidate the underlying molecular mechanism of endoplasmic reticulum (ER) stress induced delayed corneal epithelial wound healing and nerve regeneration.

Methods. Human limbal epithelial cells (HLECs) were treated with thapsigargin to induce excessive ER stress and then RNA sequencing was performed. Immunofluorescence, qPCR, Western blot, and ELISA were used to detect the expression changes of SLIT3 and its receptors ROBO1-4. The role of recombinant SLIT3 protein in corneal epithelial proliferation and migration were assessed by CCK8 and cell scratch assay, respectively. Thapsigargin, exogenous SLIT3 protein, SLIT3-specific siRNA, and ROBO4-specific siRNA was injected subconjunctivally to evaluate the effects of different intervention on corneal epithelial and nerve regeneration. In addition, Ki67 staining was performed to evaluate the proliferation ability of epithelial cells.

Results. Thapsigargin suppressed normal corneal epithelial and nerve regeneration significantly. RNA sequencing genes related to development and regeneration revealed that thapsigargin induced ER stress significantly upregulated the expression of SLIT3 and ROBO4 in corneal epithelial cells. Exogenous SLIT3 inhibited normal corneal epithelial injury repair and nerve regeneration, and significantly suppressed the proliferation and migration ability of cultured mouse corneal epithelial cells. SLIT3 siRNA inhibited ROBO4 expression and promoted epithelial wound healing under thapsigargin treatment. ROBO4 siRNA significantly attenuated the delayed corneal epithelial injury repair and nerve regeneration induced by SLIT3 treatment or thapsigargin treatment.

Conclusions. ER stress inhibits corneal epithelial injury repair and nerve regeneration may be related with the upregulation of SLIT3-ROBO4 pathway.

Keywords: endoplasmic reticulum (ER) stress, SLIT3, ROBO4, corneal epithelial wound healing, nerve regeneration

The intactness of the corneal epithelium and abundant sensory innervation are vital for maintaining normal physiological function of the cornea. Trauma, infection, dry eye syndrome (DES), and keratitis can cause damage to the corneal epithelium and nerves, and lead to visual impairment.[1,2] The regeneration of the corneal epithelium and nerves in response to injury is essential for restoring normal corneal function.

Recently, growing evidence has demonstrated the impact of endoplasmic reticulum (ER) stress in the pathogenesis of corneal epithelial – and neural defect – related diseases. ER stress is usually indicated by the level of ER stress markers, such as GRP78, XBP1, ATF6, and CHOP.[3–6] XBP1 serves as a crucial marker within the IRE1/α-XBP1 pathway of the UPR response and is essential for cell fate determination in response to ER stress.[7] CHOP maintains low levels of expression under non stress conditions; however, in ER stress response, its expression is significantly increased through IRE1-, PERK-, and ATF6-dependent transcriptional induction.[8] Inhibiting ER stress mitigates DES[9–11] and protects against alkaline burn induced corneal injuries.[12,13] One of our previous studies confirmed excessive ER stress (marked by a higher level of XBP1 and CHOP expression) in the process of corneal wound healing in diabetes; specifically, inhibiting ER stress with 4-phenylbutyric acid (4-PBA) significantly accelerates corneal epithelial and nerve regeneration.[14] Although the primary downstream mechanisms are considered to be excessive inflammation and programmed cell death triggered by ER stress, the underlying molecular mechanism of ER stress affecting corneal epithelial and nerve repair have not been elucidated.

Investigative Ophthalmology & Visual Science

Axon guidance molecules (AGMs), mainly including the slit, netrin, ephrin, and semaphorin families, are known to regulate axonal growth during development[15–18] and have been shown to play a crucial role in corneal wound healing.[19,20] Victor H. Guaiquil et al. found that following corneal epithelial injury, many AGMs, such as semaphorins, ephrins, and netrins, decreased and then quickly recovered; moreover, corneal epithelial wound healing could be promoted by semaphorin3A (Sema3A), ephrinB2 and netrin-4.[21] Semaphorin3C (Sema3C) and its receptor, neuropilin-2 (NRP-2), as well as netrin-1 and its receptor, adenosine2B, accelerates corneal epithelial and nerve regeneration.[22,23] By contrast, ephrinA1 and ephrinA2 receptor signaling restrict corneal epithelial wound healing.[24] These studies indicate that AGMs play a complex role in corneal regeneration.

The Slit guidance ligand (SLIT) family, including SLIT1, SLIT2, and SLIT3, is a secretory family. These proteins function by interacting with Roundabout receptors (ROBO) receptors (ROBO1, ROBO2, ROBO3, and ROBO4). The SLIT/ROBO signal was first discovered in the nervous system, capable of regulating axonal guidance and remnants. Recently, more and more studies have shown that the SLIT/ROBO signal can also regulate other physiological and pathological processes, such as angiogenesis, inflammatory cell chemotaxis, tumor cell migration and metastasis, fibrosis, etc.[25,26] Research in fruit flies found that JNK mediated Slit-Robo2 signaling promotes epithelial wound healing.[27] In addition, a study in diabetic mice found that SLIT2 promotes the regeneration of the corneal epithelium and nerves.[28]

In the present study, we induced ER stress in human limbal epithelial cells (HLECs) using thapsigargin (TG) and performed RNA sequencing to identify potential key molecules involved in ER stress affecting corneal regeneration. We found that ER stress caused significant changes in AGMs, with SLIT3 and its receptor, ROBO4, being particularly elevated. Therefore, in the present study, we investigated the role of ER stress in regulating corneal epithelial and nerve regeneration through the SLIT3-ROBO4 pathway.

Materials and Methods

Animals

Male C57BL/6J mice (8–10 weeks old) were obtained from Vital River Laboratory Animal Technology Co., Ltd. (Beijing, China). All animal experiments were conducted according to the guidelines and statements of the American Society for Visual and Ophthalmic Research regarding the use of animals in ophthalmic and visual research and were approved by the ethics committee of the Shandong Eye Institute. The anesthetized mice were injected subconjunctivally with 5 µL of TG (50 µm/mL), a classic ER stress agonist (MedChemExpress, Monmouth Junction, NJ, USA), or SLIT3 (100 ng/mL; R&D Systems, Minneapolis, MN, USA) 24 hours before and 0 hours after corneal epithelial scraping. ROBO4-specific siRNA (20 mmol/L), SLIT3-specific siRNA (20 mmol/L; GenePharma Company, Suzhou, China) or nonspecific control (NC) siRNAs were injected 24 hours and 4 hours before and 0 hours after wounding. The SLIT3 and ROBO4-specific siRNA sequence listed in Table 1 were synthesized using GenePharma.

Corneal Epithelial Wound Healing

The mice were administered general anesthesia through an intraperitoneal injection of 0.6% pentobarbital sodium, followed by the topical application of proparacaine hydrochloride eye drops. A 2.5 mm diameter area of the central corneal epithelium was scraped using an electric handheld epithelial scraper (Alger Co., Lago Vista, TX, USA). Subsequently, ofloxacin eye ointment was used to prevent infection. The wound healing progression was monitored using fluorescein sodium staining, and photographs were taken with a slit lamp microscope (Topcon, Tokyo, Japan). The image analysis software ImageJ was used to measure the corneal epithelial defect area in each group.

Cell Culture and Treatment

The corneal ring left over from corneal transplantation surgery in the eye bank was used for the primary culture of HLECs. The limbal corneal epithelium was removed after being digested with 15 mg/mL dispase II (Roche, Indianapolis, IN, USA) in Dulbecco's modified Eagle's medium (DMEM; Invitrogen, Carlsbad, CA, USA) overnight at 4°C. Next, the epithelium was digested into single cells using 0.25% trypsin / 0.02% EDTA at 37°C for 15 minutes. The cells were subsequently suspended in DMEM/F-12 medium supplemented with 10% fetal bovine serum (Gibco, Grand Island, NY, USA), insulin-transferrin-selenium (Invitrogen), 1% nonessential amino acids (Invitrogen), 0.1 nM cholera toxin (Sigma, St. Louis, MO, USA), 2 nM 3,3′,5-triiodo-l-thyronine sodium salt (Sigma), 0.4 ng/mL dexamethasone sodium phosphate (Wako, Osaka, Japan), 2 mM l-glutamine (Invitrogen), penicillin-streptomycin (Hyclone, Logan, UT, USA), 10 ng/mL recombinant human epidermal growth factor (EGF; R&D Systems), and 10 µM Y27632 (stem cells). The primary cells were cultured on dishes coated with a 3T3 feeder layer and passaged after 80% to 90% confluence. The passaged HLECs were treated with or without 400 nm/mL TG for 24 hours.

A mouse corneal epithelial stem/progenitor cell line (TKE2) was provided by Dr. Tetsuya Kawakita of Keio University (Tokyo, Japan). Mouse TKE2 has been applied

Table 1. Mouse SLIT3 and ROBO4 siRNA Sequences

	Forward Primer (5′–3′)	Reverse Primer (5′–3′)
SLIT3 siRNA1	CUGGACAGAAAUAACAUCATT	IGAUGUUAUUUCUGUCCAGTT
SLIT3 siRNA2	GCUGGCUUAAGUUCUGUGATT	UCACAGAACUUAAGCCAGCTT
SLIT3 siRNA3	GUGUGAGACAAACAACGAUTT	AUCGUUGUUUGUCUCACACTT
SLIT3 siRNA4	CAUGCAGUAAUAACAUUGUTT	ACAAUGUUAUUACUGCAUGTT
ROBO4 siRNA1	GGCCAAGACUAUGAAUUCATT	UGAAUUCAUAGUCUUGGCCTT
ROBO4 siRNA2	GCUGCUACUAGGCAUUACUTT	AGUAAUGCCUAGUAGCAGCTT
ROBO4 siRNA3	CAGCUUCUGAGGACAAUGUTT	ACAUUGUCCUCAGAAGCUGTT
ROBO4 siRNA4	CAACAACCUAUGGCUAUAUTT	AUAUAGCCAUAGGUUGUUGTT

Table 2. The Antibodies Used in the Experiment

Antibodies	Supplier	Code
Ki67	Abcam	ab16667
SLIT3	Affinity	DF9909-100
ROBO4	Affinity	DF14939
TUBB3	Biolegend	657404
CHOP	Affinity	AF6277
XBP1	Proteintech	24868-1-AP
Alexa Fluor 488	Invitrogen	A-21206
Alexa Fluor 488	Invitrogen	A-21202

in the research of cell biology of corneal epithelial cells.[29–32] The mouse TKE2 cells were cultured in KSFM basal medium (Gibco/Thermo Fisher Scientific Inc., Waltham, MA, USA) supplemented with human keratinocyte growth supplement (HKGS; Gibco) and recombinant human EGF (5 ng/mL; R&D Systems) at 37°C with 5% CO_2. This cell line has been characterized in our previous studies.[33,34] Finally, the TKE2 cells were treated with recombinant at a concentration of 100 ng/mL SLIT3 or 400 nm/mL TG.

Cell Proliferation and Migration Analysis

To detect the effect of TG on the proliferation of HLECs or mouse TKE2 cells, the cells were digested into single cells using 0.25% trypsin / 0.02% EDTA after 24 hours of treatment of TG, and the cell number was counted. To detect the effect of SLIT3 on the proliferation of mouse TKE2 cells, the latter were treated with SLIT3 protein at a final concentration of 100 ng/mL for 24 hours and measured using a CCK-8 assay kit (Bioss, Beijing, China).

For the migration assay of mouse TKE2 cells, the cells were cultured to confluence and scraped with a 200 µL pipette tip. Subsequently, the cells were washed 3 times with phosphate-buffered saline (PBS), and exogenous SLIT3 protein was added at a final concentration of 100 ng/mL. Photographs of the samples were taken after 0 hours and 24 hours, and the percentage of the closed area was calculated using ImageJ.

Immunofluorescence Staining

For immunofluorescence staining, a frozen section (7 µm) of the treated cells was fixed in 4% paraformaldehyde for 20 minutes at room temperature, permeabilized, and blocked for 1 hour in PBS using 5% BSA and 0.1% Triton X-100, followed by primary antibody incubation overnight at 4°C. The samples were then incubated with a fluorescein-conjugated secondary antibody for 2 hours at room temperature. The proportion of Ki67-positive cells in the corneal limbus and wound margin was calculated by counting the number of Ki67 positive–stained cells and DAPI-stained cells. The relative expression of CHOP, XBP1, SLIT3, and ROBO4 was calculated by performing a quantitative analysis of the fluorescence intensity using ImageJ. The antibodies used in this assay were shown in Table 2.

Whole-Mount Staining of Corneal Nerves

For corneal whole-mount staining, the corneas were dissected and fixed with 4% paraformaldehyde for 1 hour at 4°C. The corneas were permeabilized and blocked with PBS containing 0.3% Triton X-100 and 5% BSA overnight at 4°C, and then incubated with TUBB3 antibodies overnight. The staining was observed and captured using a ZEISS confocal microscope (ZEISS, Jena, Germany), and the nerve density was calculated using ImageJ.

RNA Sequencing

After 24 hours of culture with TG-treated or without TG-treated HLECs, the cells were collected and sent to a biotech company (Oebiotech Biomedical Technology Co., LTD., Shanghai, China) for RNA sequencing. The sequencing was performed using the Illumina HiSeq 4000 high-throughput sequencing platform. Finally, GSEA, volcano plot, and heat map analyses were conducted using oebiotech.com.

Reverse Transcription Quantitative PCR

Complete RNA was extracted using a TransZol Up Plus RNA kit (Transgen Biotech, Beijing, China). The cDNA was synthesized by reverse transcription using complementary DNA and using a HiScript III RT SuperMix Kit (R323-01; Vazyme, Nanjing, China). A ChamQ Universal SYBR qPCR Master Mix (Vazyme Biotech Co., Ltd., Nanjing, China) and a Rotor-Gene Q Real-Time PCR cycler (Qiagen, Germany) were used to perform real-time PCR. The primers listed in Tables 3 and 4 were synthesized using GenePharma. The expression of human and mouse β-actin was used for normalization to calculate the mRNA levels of each sample. The $2^{-\Delta\Delta}$ct method was used to analyze the relative expression levels of mRNA.

ELISA Analysis

After 24 hours of treatment with or without TG, the mouse TKE2 cells were collected. After thorough lysis, centrifugation was performed at 3000 rpm for 10 minutes, and the supernatant was collected. The concentration of SLIT3 protein was determined using the Mouse SLIT3 ELISA Kit according to the instructions (FanKeW, Shanghai, China).

Table 3. Mouse Primer Sequences Used for qPCR

Genes	Forward Primer (5′–3′)	Reverse Primer (5′–3′)
Slit1	GTCAGTGCCCCCTGCAGTAC	TGTCACCCGTGTAACCTAGCAT
Slit2	GCGAGTTCGAGCCAGCTATG	ACTTTAGGGCTTCCTCCATCCA
Slit3	GCCAAAGGATGTGACTGAACTGTA	GTGGGACATGTTGCTGAAGGT
Robo1	CGCCTCCTGAAGACACACAA	ACACTGTATCGGATCCCAGGAA
Robo2	TTCTTCCTGCAAGCGCGTAT	TGATCGCTCTGACCATAAACAAG
Robo3	GGAATAGCTGGCTTAGGAAGCA	GTGGCCCCAGACTGTGGAT
Robo4	TCGTGGAGCTTCCAGTCATG	GGGCTAGGACAGGAGAGGAAAG
β-Actin	ACGGCCAGGTCATCACTATTG	AGAGGTCTTTACGGATGTCAACGT

Table 4. Human Primer Sequences Used for qPCR

Genes	Forward Primer (5′–3′)	Reverse Primer (5′–3′)
SLIT1	GCGGCTATAAGGGTCGAGACT	TGTTCACCCCACAGGTTGGT
SLIT2	GGTGAACACTGCGACATCGA	GAGGACCATGGGTGGAGAAA
SLIT3	GAGAGGGAGCTTTCGATGGA	GTCATTACTCACACAGCCGATCA
ROBO1	TAGTTCTTCGGACGGCTCCTT	GTGGGCCTAGGGCACTGA
ROBO2	TCCATGGCTTGCTGATTCTTG	CCATCTGAGAGCATCGTTGCT
ROBO3	GCCAGTACGCTCCTCCAGAGT	CTAGGCAGCTCAGTTCACAAGAAG
ROBO4	GCAGCTGAGGGCTACCTTGA	CTGTGATCCATCCTGTGTTTTAGG
β-ACTIN	GGGAAATCGTGCGTGACATT	GGAACCGCTCATTGCCAAT

Measurements were taken at an absorbance of 450 nm using a microplate reader (Molecular Devices, Sunnyvale, CA, USA).

Western Blot

The supernatant from mouse corneal epithelium after lysis and centrifugation were collected and used for Western blot detection. Then, 50 µg of protein were electrophoresed on a 7.5% SDS-PAGE gel, and then transferred to a polyvinylidene fluoride (PVDF) membrane (Millipore, Billerica, MA, USA). The PVDF membrane was blocked with 5% skim milk at room temperature for 2 hours. TBST was used for 3 times of washing, each for 10 minutes, followed by overnight incubation with anti-ROBO4 antibody (1:2000; Affinity, Jiangsu, China) at 4°C. On the next day, the membrane was incubated for 2 hours at room temperature with an HRP-conjugated secondary antibody (1:4000; Proteintech, Shanghai, China). The blots were visualized using the Bio-Rad Molecular Imager Che-miDoc XRS system (Bio-Rad Laboratories, Inc., Hercules, CA, USA). Nonmuscle β-actin (1:4000; Proteintech, Shanghai, China) was used as a loading control.

TUNEL Assay

To detect the cells death levels in TG treated mouse cornea, HLECs, and mouse TKE2 cells, we used a in situ cell death detection kit (Roche Applied Science, Penzberg, Upper Bavaria, Germany) and performed as per the manufacturer's instructions.

Statistical Analysis

Statistical analysis was performed using GraphPad Prism 8 (GraphPad Software Inc.). The data are presented as mean ± SD. Paired *t*-tests were utilized to compare differences between the two groups, whereas an analysis of variance (ANOVA) was used to compare differences among three or more groups. Each experiment was repeated at least three times to ensure reproducibility.

Results

TG-Induced ER Stress–Impaired Corneal Epithelial and Nerve Regeneration

To evaluate the pathological effects of ER stress after corneal injury, we induced corneal ER stress by subconjunctivally injecting TG, a commonly used ER stress inducer. Here, we found that TG induced higher expression levels of ER stress markers *Xbp1* and *Chop* in corneal epithelium (Supplementary Figs. S1A–S1C). We found that the healing of the corneal epithelium was significantly suppressed by TG treatment (Fig. 1A). Compared with normal corneas, the healing rates decreased by 34.76 ± 8.62% and 16.56 ± 1.53% 24 hours and 36 hours after injury, respectively (Fig. 1B). The Ki67-positive cells in the limbus and central wound margin were markedly reduced in the TG-treated corneas during wound healing (Figs. 1C, 1D). In addition, we performed corneal nerve whole-mount staining and found that TG significantly hindered the repair of the corneal nerves (Fig. 1E, Supplementary Figs. S2A, S2C). The peripheral nerve density of TG treated corneas decreased by 85.79 ± 0.54%, 45.13 ± 1.73%, and 12.64 ± 0.95% and the central nerve density of TG treated corneas decreased by 100%, 74.87 ± 2.13%, and 19.34 ± 1.64% compared with normal corneas at 24 hours, 5 days and 30 days after epithelial scraping, respectively (Fig. 1F, Supplementary Figs. S2B, S2D). These results demonstrated that TG-induced ER stress directly impaired both corneal epithelial wound healing and nerve regeneration. By the way, although significantly delayed compared to the control group, after TG treatment, the defect of corneal epithelium was closed at 48 hours after scraping and the nerves were gradually recovering.

TG-Induced ER Stress Inhibited the Proliferation Ability of HLECs and Mouse TKE2 Cells

The primary cultured HLECs and mouse TKE2 cells were treated with 400 nm TG for 24 hours, and the mRNA expressions of ER stress associated genes XBP1 and CHOP were found to be upregulated (see Supplementary Figs. S1D, S1E). We observed that TG caused an obvious change in cell morphology, from regular cobblestone-like shapes to irregular shapes (Fig. 2A). Cell counting revealed that TG significantly reduced the number of cells (Fig. 2B). The proliferation marker of Ki67 staining showed that the Ki67 positive cells were reduced dramatically in HLECs after TG treatment (Figs. 2C, 2D). Similar changes in cell morphology and decreased proliferation were also observed in mouse TKE2 cells after TG treatment (Figs. 2E–H). These findings suggested that TG-induced ER stress impaired the growth ability of corneal epithelial cells. Here, we used TUNEL staining analysis to evaluate the programmed cell death level of TG treated corneal epithelial cells. We found that TG induced cell death in wounded corneas, however most of the TUNEL positive cells were distributed in the corneal stroma (Supplementary Fig. S3A). After 24 hours of TG treatment, no TUNEL positive apoptotic cells were found in both HLECs and mouse TKE2 cells (Supplementary Figs. S3B, S3C). KEGG analysis of transcriptome data revealed that genes downregulated by TG in HLECs exhibit a high enrichment of cell cycle related genes (Supplementary Fig. S3D), suggesting that under the concentration and treatment time

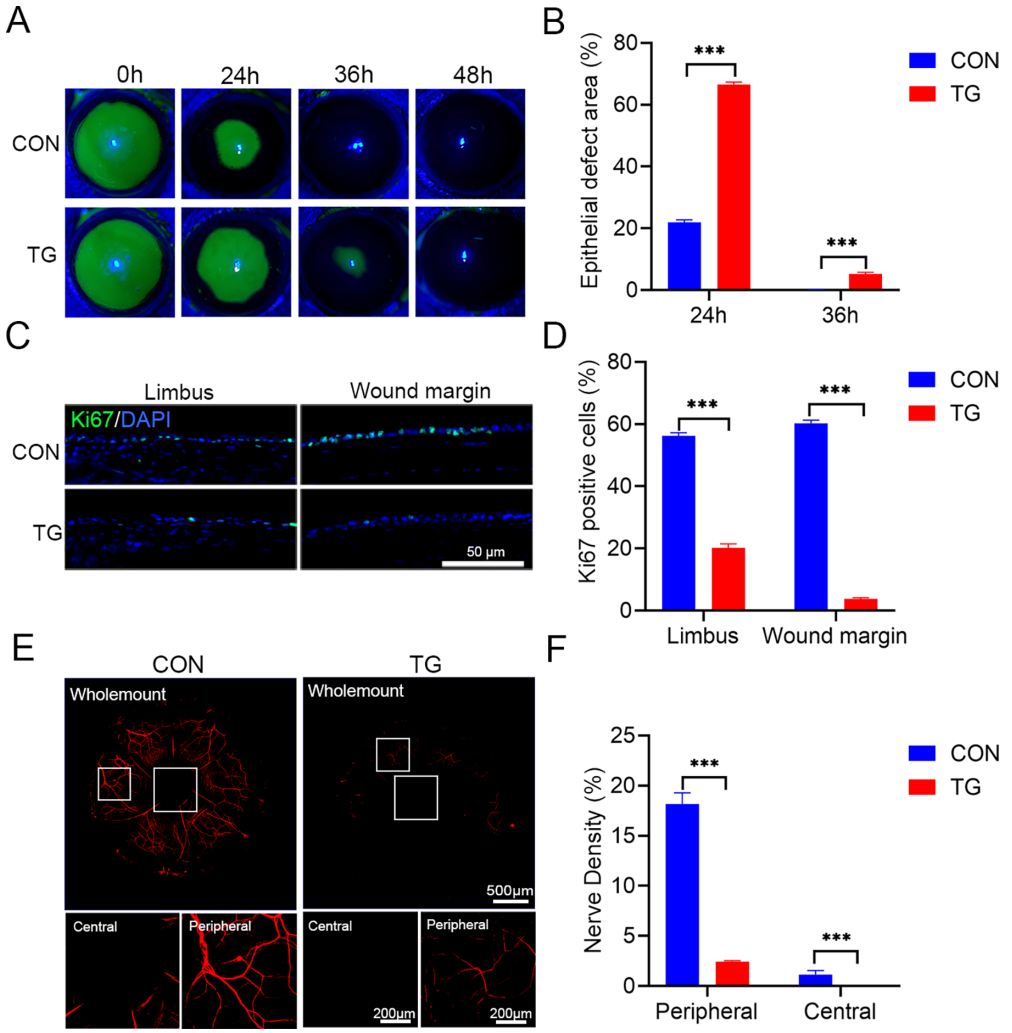

Figure 1. TG-induced ER stress inhibited corneal epithelial and nerve regeneration. (**A**) After epithelial scraping, the remaining wound defect was stained with fluorescein sodium and photographed at 0 hours, 24 hours, 36 hours, and 48 hours. (**B**) The epithelial defects at 24 hours and 36 hours were quantified as the percentage of defect area relative to the original wound area (n = 4/group). (**C**) Ki67-staining of corneas of the control and TG-treated groups 24 hours after injury. (**D**) The percentage of Ki67-positive cells (%) at the limbus and wound margin was calculated (n = 4/group). (**E**) Whole-mount corneal staining of TUBB3 24 hours after epithelial scraping; the representative areas of the central and peripheral corneas are presented below. (**F**) Statistics of nerve density in central and peripheral corneas in the control and TG-treated groups 24 hours post-wounding using ImageJ (n = 4/group). ***P < 0.001.

of this experiment, TG may inhibit cell growth by affecting the cell cycle.

TG-Induced ER Stress Upregulated SLIT3 and ROBO4 Signaling in HLECs

To further investigate the potential molecular mechanism, we conducted RNA sequencing. The GSEA analysis, a powerful analytical method that compares gene sets across biological states and detects statistically significant differences,[35] confirmed that TG induced an excessive ER stress response in HLECs (Fig. 3A). Subsequently, according to KEGG analysis, we focus on the differential genes related with development and regeneration. We found that axon guidance–related genes constituted a substantial portion, with significant upregulation of SLIT3 expression (Fig. 3B). A volcano plot illustrating SLIT–ROBO signaling showed significant upregulation of SLIT3 and ROBO4 expression (Fig. 3C). We then performed qPCR to test the expression of *SLIT1–3* and *ROBO1–4*, and the results were consistent with the RNA sequencing data: significant upregulation of *SLIT3* and *ROBO4* in the TG-treated group was observed (Figs. 3D, 3E).

TG-Induced ER Stress Increased SLIT3 and ROBO4 Expression in Mouse TKE2 Cells and Wounded Mouse Corneal Epithelium

We verified whether TG can also induce upregulation of the Slit3-Robo4 pathway in mouse TKE2 cells. The qPCR and immunofluorescence staining results showed that the mRNA and protein level of *Slit3* and *Robo4* in TG-treated mouse TKE2 cells were upregulated markedly (Figs. 4A–C). In addition, through ELISA assay, we found that the concentration of SLIT3 in the lysis solution of TG treated mouse TKE2 cells was increased significantly (Fig. 4D). To detect the effect of ER stress on SLIT3 and ROBO4 expression during corneal

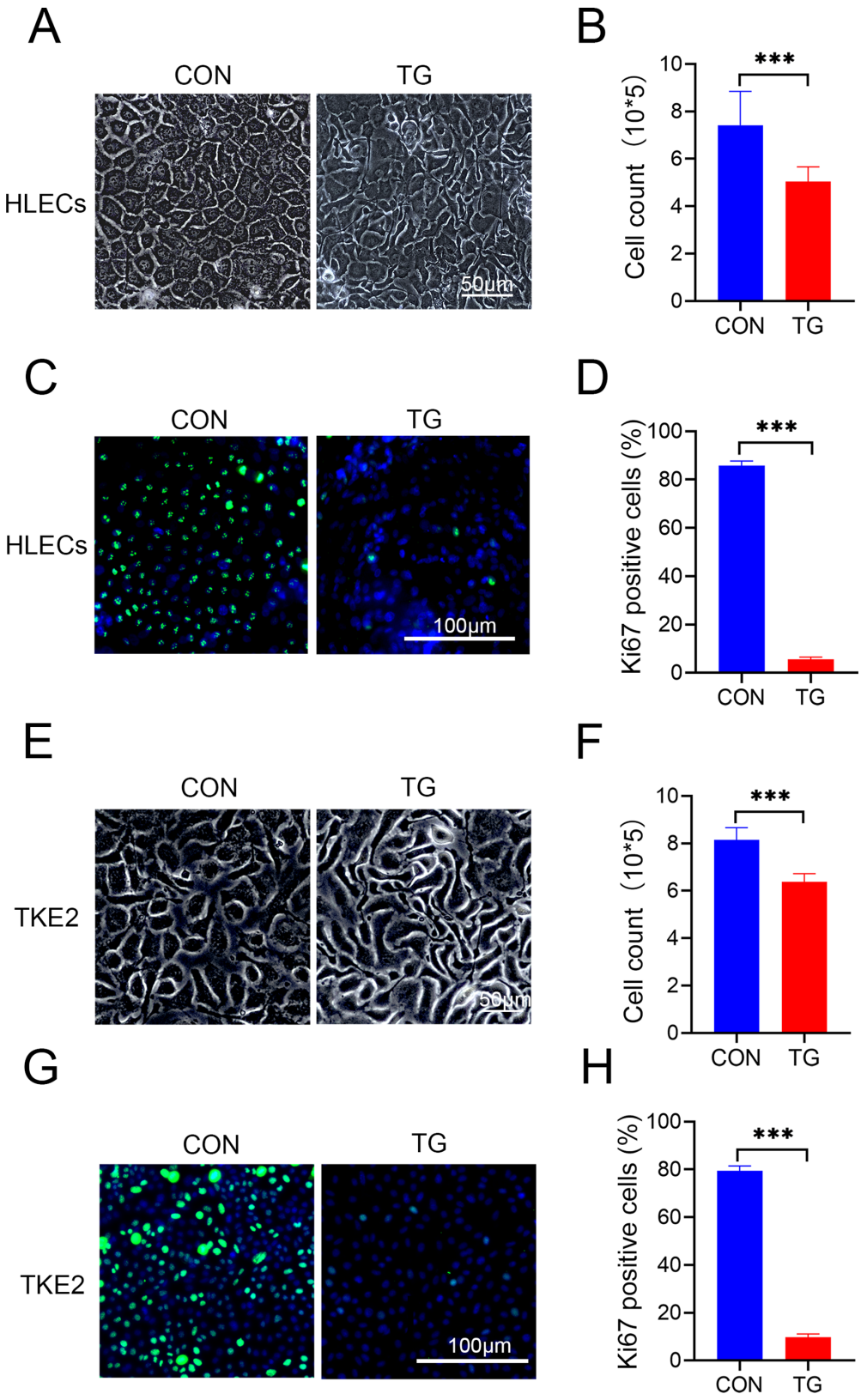

Figure 2. Effects of TG-induced ER stress on HLECs and mouse TKE2 cells growth. (**A**) Morphological changes in HLECs under light microscopy after the induction of ER stress. (**B**) Cell count statistics of HLECs after TG treatment for 24 hours ($n = 4$/group). (**C**) Ki67-staining of HLECs of the control and TG-treated groups after 24 hours. (**D**) The number of Ki67-positive cells at HLECs was calculated and represented as a percentage of Ki67-positive cells (%; $n = 4$/group). (**E**) Morphological changes in mouse TKE2 cells under light microscopy after the induction of ER stress ($n = 4$/group). (**F**) Cell count statistics of mouse TKE2 cells after TG treatment for 24 hours. (**G**) Ki67-staining of mouse TKE2 cells of the control and TG-treated groups after 24 hours. (**H**) The number of Ki67-positive cells at mouse TKE2 cells was calculated and represented as a percentage of Ki67-positive cells (%; $n = 4$/group). ***$P < 0.001$.

Investigative Ophthalmology & Visual Science

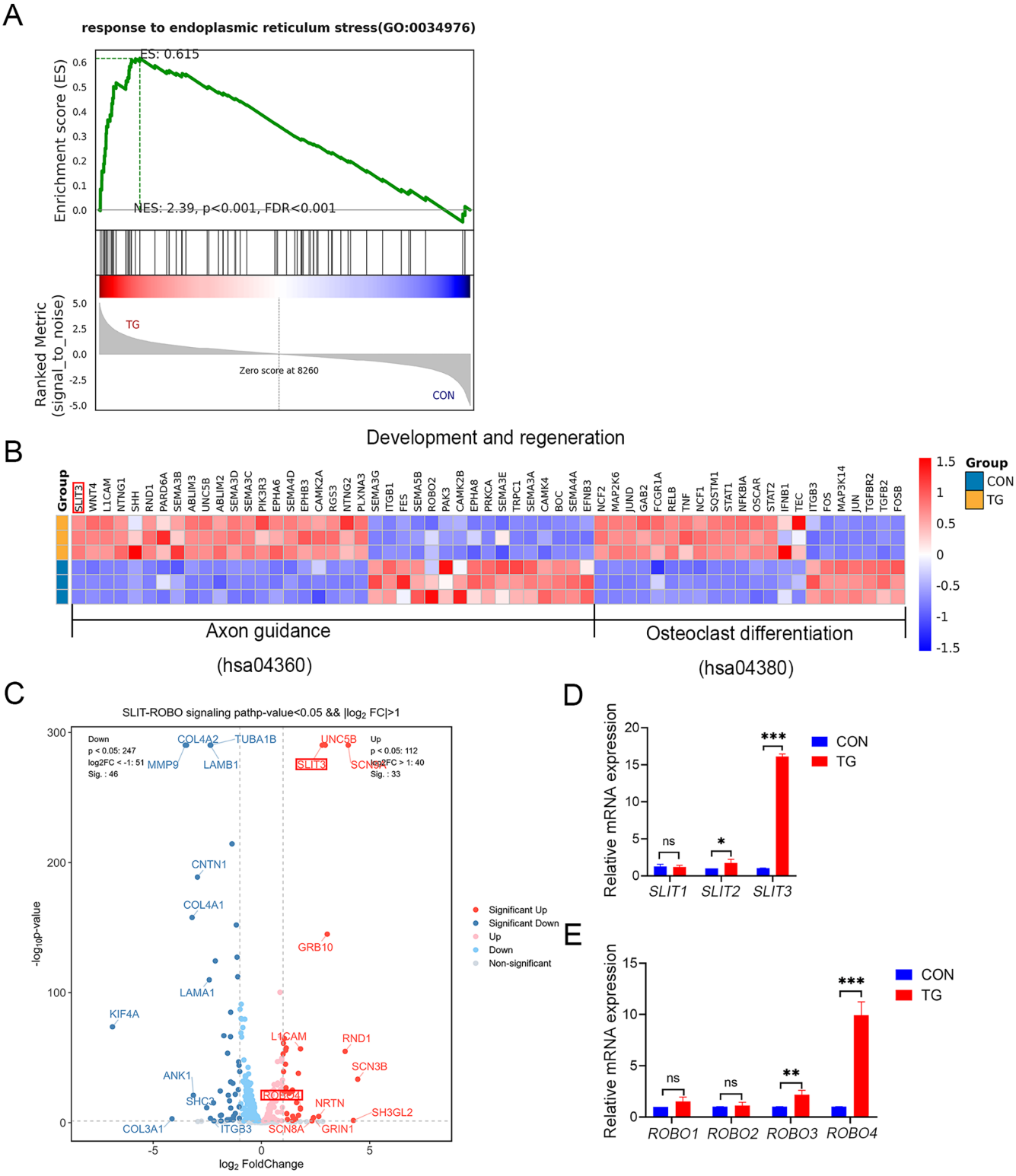

Figure 3. Transcriptional profiling of HLECs subjected to ER stress. (**A**) Gene set enrichment analysis (GAES) of ER stress response–related genes. (**B**) Heat map of genes related to development and regeneration according to KEGG analysis. (**C**) Volcano plot of RNA sequencing data comparing the SLIT–ROBO signaling pathway–related gene transcripts in the control and TG-treated HLECs. The *red dots* represent upregulated genes, and the *blue dots* represent downregulated genes; adjusted $P < 0.05$ and $|\log2FC| > 1$. (**D, E**) The qPCR detection of mRNA expression of *SLIT1–3* and *ROBO1–4*. ns, not significant; $^{*}P < 0.05$; $^{**}P < 0.01$; $^{***}P < 0.001$. $n = 3$/group for RNA sequencing.

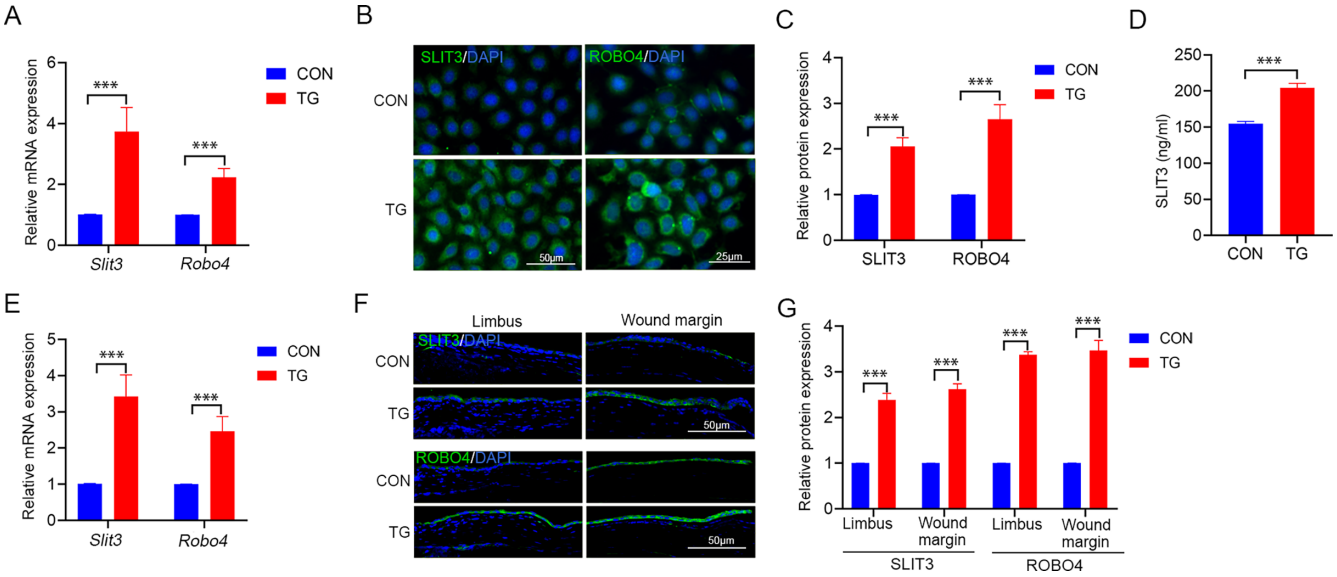

Figure 4. TG treatment upregulated the expression of SLIT3 and ROBO4 in mouse TKE2 cells and wounded corneas. (**A**) The qPCR detection of *Slit3* and *Robo4* mRNA expression in mouse TKE2 cells after TG treatment ($n = 3$/group). (**B, C**) After 24 hours of treatment, the cells were collected for SLIT3 and ROBO4 staining and the relative protein expression of SLIT3 and ROBO4 were analyzed ($n = 4$/group). (**D**) The protein concentration of SLIT3 in mouse TKE2 cells lysis solution was detected through ELISA ($n = 3$/group). (**E**) Relative mRNA expression of *Slit3* and *Robo4* in mouse wounded corneal epithelium with or without TG treatment 24 hours after epithelial scraping. (**F, G**) Representative images of SLIT3 and ROBO4 staining in wounded corneas of control and TG-treated mice at 24 hours post-wounding and the relative protein expression in limbus and wound margin were analyzed ($n = 4$/group). ***$P < 0.001$.

wound healing in vivo, healed corneas with or without TG treatment were collected at 24 hours post-wounding and subjected to qPCR and immunofluorescence staining. The results indicated that TG treatment induced higher mRNA and protein expression of SLIT3 and ROBO4 in the epithelium of wounded corneas (Figs. 4E–G).

Application of SLIT3 Delayed Corneal Epithelial and Nerve Regeneration

To explore the effect of SLIT3 on corneal epithelial repair and nerve regeneration, we performed corneal epithelial curettage in mice subconjunctivally injected with recombinant SLIT3 protein. The unhealed areas in exogenous SLIT3–treated corneas were larger than those in normal corneas, as shown in Figure 5A. The epithelial defect areas in the normal and SLIT3-treated groups were 30.25 ± 0.75% and 62.26 ± 8.15% at 24 hours and 0.78 ± 0.52% and 6.58 ± 1.70% at 36 hours after wounding, respectively (Fig. 5B). On the contrary, inhibition of SLIT3 by application of SLIT3-specific siRNA partially reversed TG-induced delayed of corneal wound healing (Figs. 6A, 6B). Compared with the untreated group, the proportion of Ki67-positive cells in the limbus and wound margin of the SLIT3-treated group were decreased significantly (Figs. 5C, 5D), indicating a reduction in proliferation ability due to SLIT3.

The proliferation and migration abilities of cells are crucial for epithelial wound healing, here, we studied the effect of SLIT3 on the proliferation and migration in mouse TKE2 cells. The CCK8 detection results showed that SLIT3 significantly decreased the proliferation ability of mouse TKE2 cells (Supplementary Fig. S4A). Consistently, the proliferation marker of Ki67 expression in SLIT3 treated group was reduced (Supplementary Figs. S4B, S4C). Next, a scratch experiment was performed to verify the effect of SLIT3 and TG on cell migration. Compared to the control group, SLIT3-treatment inhibited the cell migration significantly, and TG treatment with or without SLIT3 almost completely blocked the migration ability of cells (see Supplementary Figs. S4D, S4E).

We further examined TUBB3 staining 24 hours and 5 days after epithelial scraping and found that SLIT3 inhibited nerve regeneration (Fig. 5E, Supplementary Fig. S5A). SLIT3 reduced the nerve density in the peripheral cornea by 58.98 ± 2.87% and 46.61 ± 1.52% 24 hours and 5 days after injury, respectively; and SLIT3 reduced the nerve density in the central cornea by 100% and 75.25 ± 2.89% 24 hours and 5 days after injury, respectively (Fig. 5F, Supplementary Fig. S5B). These findings proved that SLIT3 suppressed the regeneration of the corneal epithelium and nerves dramatically, similar with the effects of TG.

ROBO4 Receptor Mediated the Inhibitory Effect of TG and SLIT3 on Corneal Epithelial and Nerve Regeneration

SLIT3 treatment dramatically enhanced the mRNA and protein level of ROBO4 in mouse corneal epithelium wound healing (Supplementary Figs. S6A–S6C) and in cultured mouse TKE2 cells (Supplementary Figs. S6D–F). To verify whether TG induced ER stress increases ROBO4 levels through SLIT3, the SLIT3-specific siRNA was used. The results showed the enhancement of SLIT3 and ROBO4 induced by TG was significantly inhibited by SLIT3-specific siRNA (Fig. 6C), indicating that TG promotes the increase of ROBO4 expression through SLIT3.

To demonstrate that ER stress–induced SLIT3 exerts inhibitory effects on corneal repair through its recep-

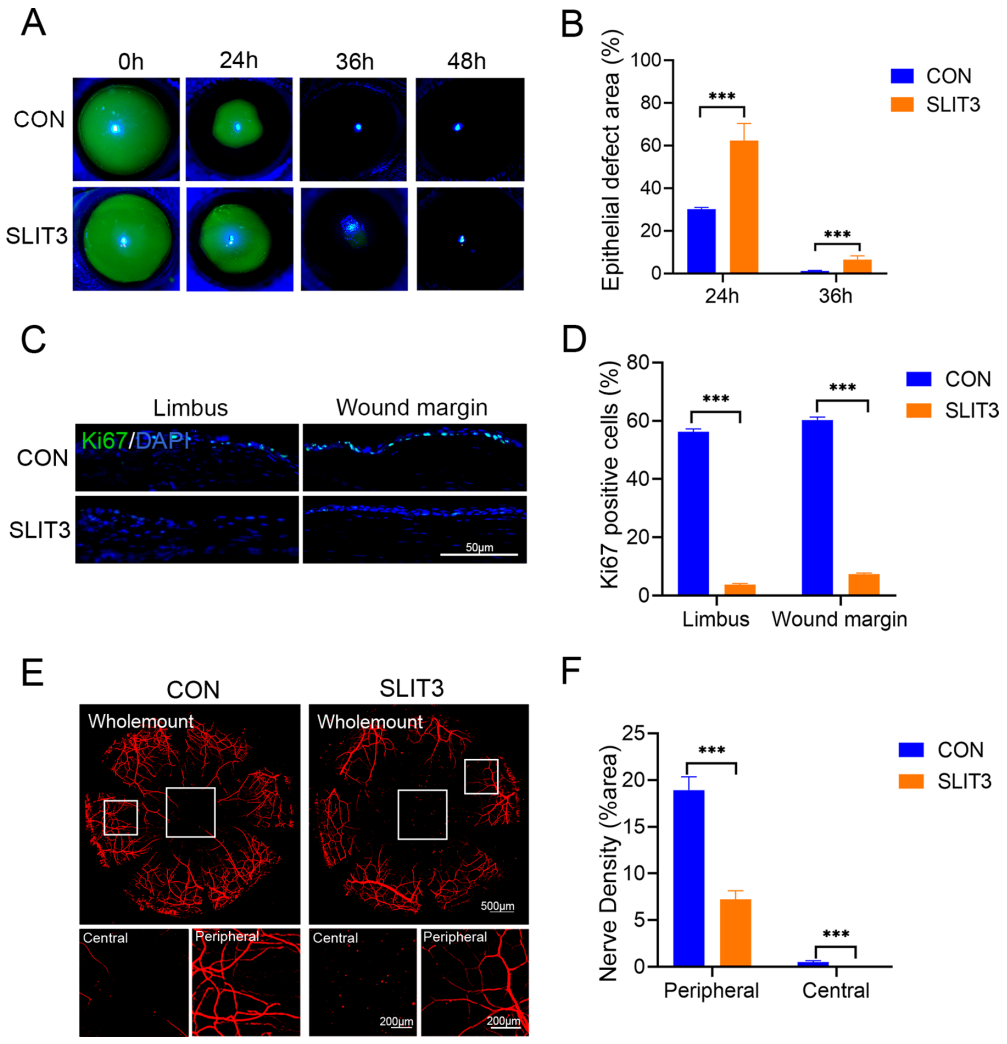

Figure 5. Effect of recombinant SLIT3 protein on corneal epithelial and nerve repair. (**A**) Subconjunctival injections of SLIT3 or control solvent were performed after scraping a 2.5 mm diameter area of the corneal epithelium. The remaining defect was stained with fluorescein sodium and photographed at 0 hours, 24 hours, 36 hours, and 48 hours after injury (n = 4/group). (**B**) Epithelial defects at 24 hours and 36 hours were quantified as the percentage of defect area relative to the original wound area. (**C**) Representative images of Ki67 staining of limbus and wound margin in the control and SLIT3-treated corneas. (**D**) The percentage of Ki67-positive cells of limbus and wound margin in the control and SLIT3-treated corneas was calculated (n = 4/group). (**E**) The corneal nerves in the control and SLIT3-treated groups were detected using whole-mount TUBB3 staining 24 hours after epithelial scraping (n = 4/group). The total (*upper*) and locally magnified (*lower*) figures are presented. (**F**) The peripheral and central nerve density in the control and SLIT3-treated groups was calculated through Image J analysis. ***$P < 0.001$.

tor ROBO4, we used specific siRNA to knock down the expression of ROBO4 in mouse corneas. Knocking down ROBO4 completely alleviated the inhibitory role of SLIT3 in epithelial repair (Figs. 7A, 7B). The effectively knocking down of ROBO4 by siRNA was demonstrated by Western blotting assay (Figs. 7C, 7D). The Ki67-staining results showed that knocking down ROBO4 significantly restored the proliferative capacity of the epithelial cells inhibited by SLIT3 (Figs. 7E, 7F). To investigate the recovery role of ROBO4 knockdown on SLIT3-suppressed nerve regeneration, we performed TUBB3 immunostaining. The results indicated that knocking down ROBO4 effectively attenuated the inhibitory effect of SLIT3 on nerve regeneration (Figs. 7G, 7H). These findings suggest that the inhibitory effects of SLIT3 on corneal epithelial and nerve regeneration were mediated through its receptor, ROBO4.

Considering that TG-induced ER stress significantly upregulated the expression of SLIT3 and ROBO4, we hypothesized that ER stress impacts corneal epithelial wound healing and nerve regeneration through the SLIT3–ROBO4 signaling pathway. To validate this hypothesis, we used ROBO4 siRNA under TG-induced ER stress. Results from the epithelial scraped assay and subsequent staining demonstrated that knocking down ROBO4 partially reversed the inhibitory effects of TG on corneal epithelial healing (Figs. 8A, 8B). Western blotting results demonstrated the effectively knocking down of ROBO4 by siRNA (Figs. 8C, 8D). TG induced Ki67 expression was reversed by ROBO4-specific siRNA (Figs. 8E, 8F). In addition, corneal peripheral nerve regeneration delayed by TG was partially recovered by ROBO4-specific siRNA (Figs. 8G, 8H). These findings indicate that ER stress inhibits corneal epithelial

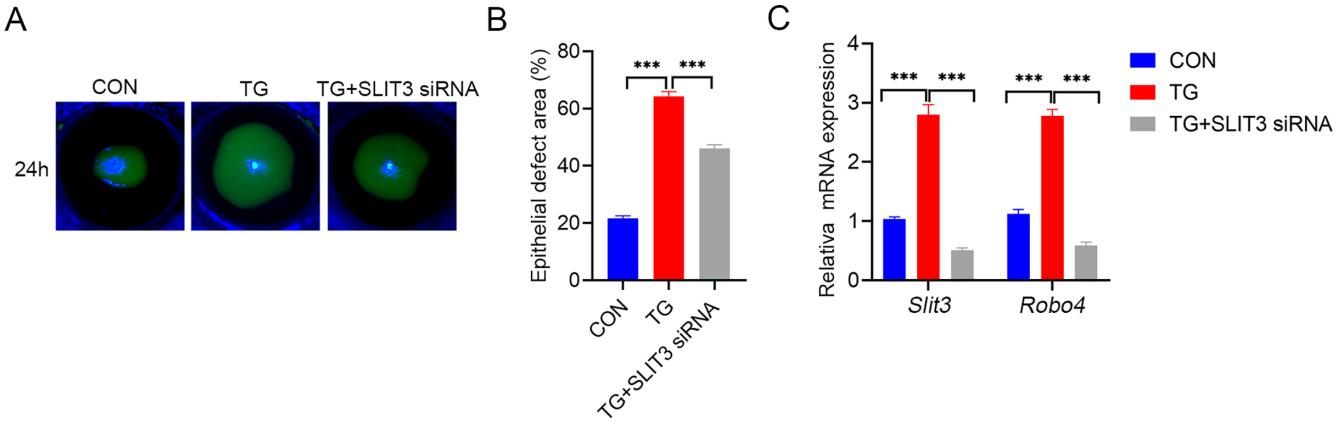

Figure 6. TG inhibited corneal epithelial wound healing through SLIT3. (**A**) SLIT3-specific siRNA partially blocked the inhibitory effect of TG on corneal epithelial wound healing ($n = 4$/group). (**B**) Epithelial defects at 24 hours were quantified as the percentage of defect area relative to the original wound area. (**C**) The qPCR detection of *Slit3* and *Robo4* in mouse wounded corneal epithelium after TG treatment ($n = 4$/group), $^{***}P < 0.001$.

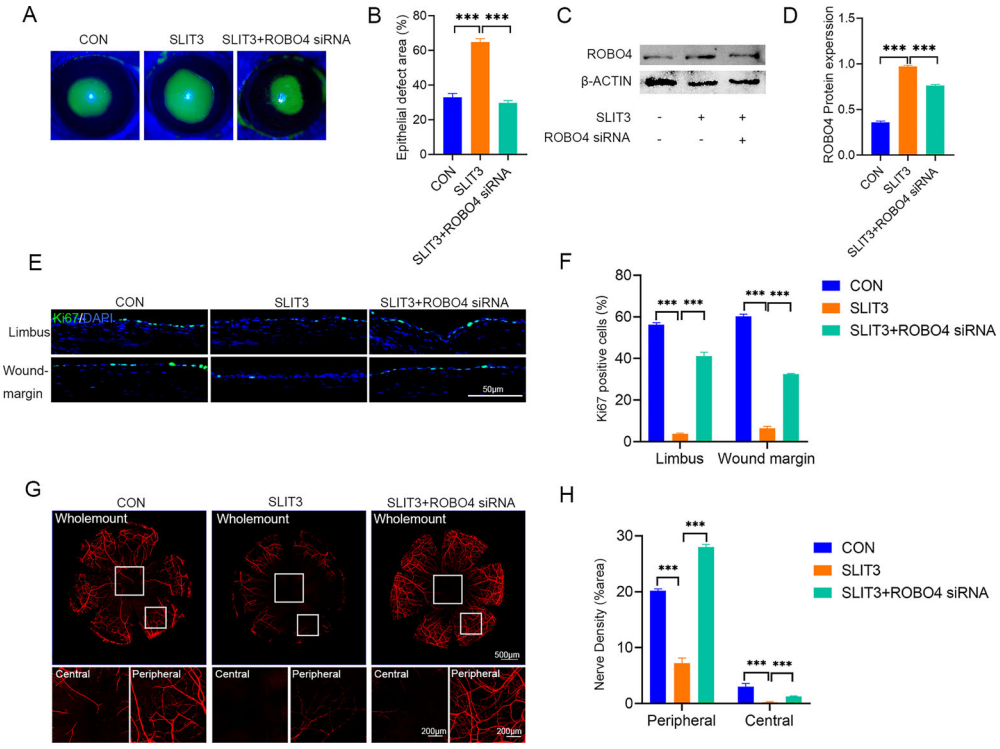

Figure 7. Effect of ROBO4 siRNA on SLIT3-inhibited corneal epithelial and nerve regeneration. (**A, B**) ROBO4-specific siRNA effectively blocked the inhibitory effect of SLIT3 on corneal epithelial wound healing ($n = 4$/group). (**C, D**) Western blot assay showed that SLIT3 induced increased ROBO4 expression was inhibited by ROBO4-specific siRNA. (**E, F**) ROBO4-specific siRNA increased the proportion of Ki67-positive cells in SLIT3-treated healing corneal epithelium ($n = 4$/group). (**G, H**) ROBO4-specific siRNA reversed the inhibitory effect of SLIT3 on nerve regeneration ($n = 4$/group). $^{***}P < 0.001$.

healing and nerve regeneration through the upregulation of the SLIT3–ROBO4 pathway to a certain degree.

By the way, the activity of four specific siRNAs for SLIT3 and ROBO4 synthesized by GenePharma was validated using a TG-treated corneal epithelial injury model, and ultimately selected SLIT3-specific siRNA4 and ROBO4-specific siRNA3, which had the most significant recovery effect on TG-inhibited corneal epithelial wound healing in the subsequent experiments (Supplementary Fig. S7).

Discussion

ER stress plays a significant role in corneal pathology, affecting the regeneration of the epithelium and nerves, but the specific molecular mechanism remains unclear.[14,36] This study aims to investigate the potential molecular mechanisms underlying the ER stress–induced delayed repair of the corneal epithelium and nerves. TG, a cell-permeable sesquiterpene lactone derived from the plant thapsiagar-

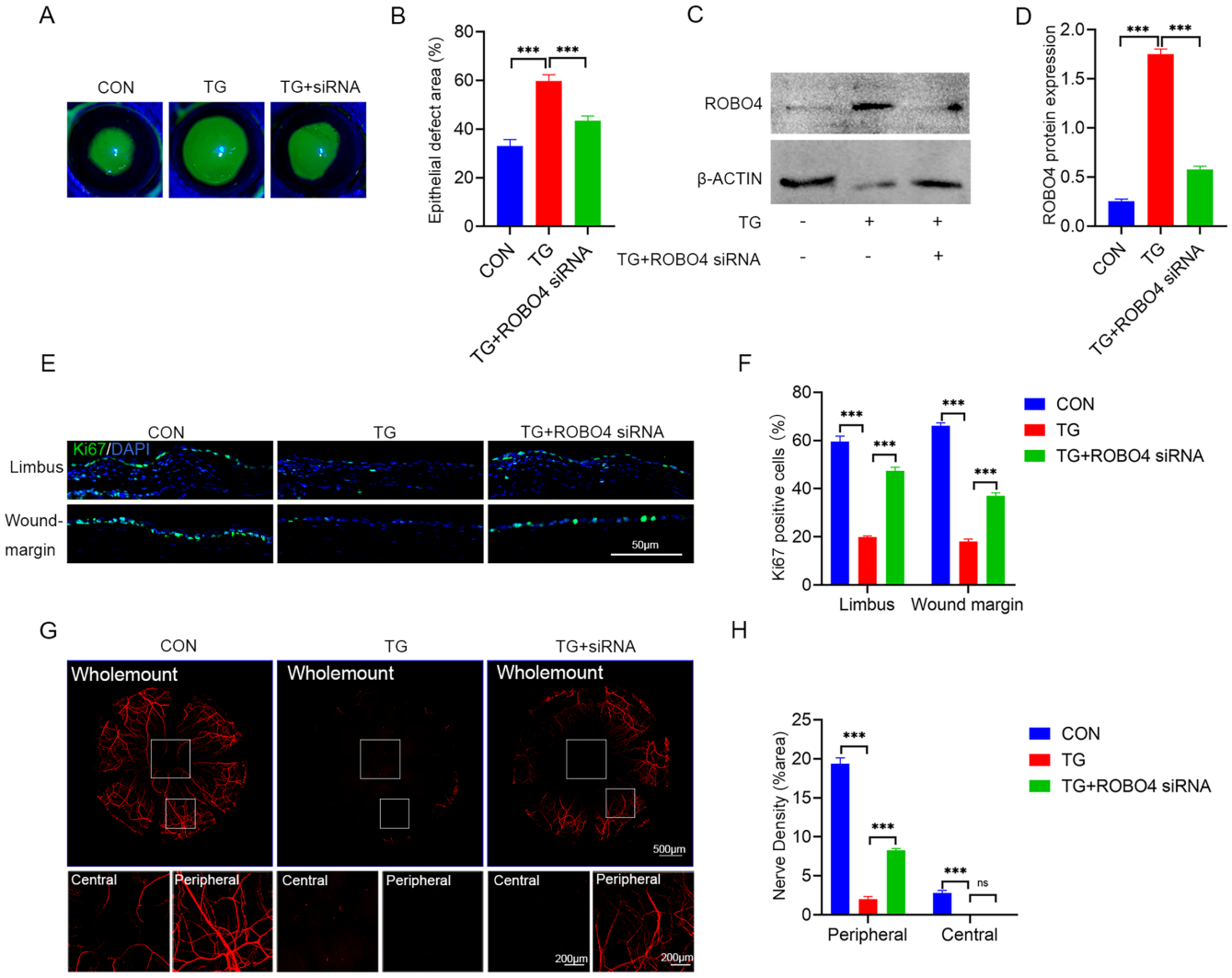

Figure 8. Effect of ROBO4 siRNA on TG-inhibited corneal epithelial and nerve regeneration. **(A, B)** The inhibition of corneal epithelial wound healing induced by TG was partially reverted by ROBO4-specific siRNA application ($n = 4$/group). **(C, D)** Western blot assay showed that application of ROBO4-specific siRNA inhibited TG induced increased ROBO4 expression. **(E, F)** The proportion of Ki67-positive cells in wounded corneal epithelium, reduced by TG, was partially restored by the application of ROBO4-specific siRNA ($n = 4$/group). **(G, H)** Peripheral corneal nerve density reduction during wound healing due to TG was partially restored by ROBO4-specific siRNA ($n = 4$/group). ***$P < 0.001$.

ganic, can induce ER stress by specifically inhibiting ER Ca^{2+}-ATPase, making it a suitable inducer for studying the mechanisms of ER stress.[37,38] Here, we induced ER stress in the cornea in vivo by subconjunctival injection of TG and found that ER stress leads to delayed wound healing in the corneal epithelium and nerve regeneration. These findings are consistent with previous research on the effects of ER stress on corneal epithelial and nerve repair.[14,39] We further induced ER stress using TG in cultured HLECs and mouse TKE2 cells. There is a correlation between the morphology and function of cells. A study showed that cell size of human corneal epithelial cells are associated with stem cell property and proliferative capacity.[40] TG treated HLECs and mouse TKE2 cells displayed irregular elongated shapes and enlarged size, which may be related to the decreased stem cell activity and proliferation ability in TG treated cells.

To gain more insight into the mechanism of ER stress intervention in regeneration, we performed RNA sequencing on cells with or without TG treatment. Through KEGG analysis, we found that the genes related to development and regeneration were mainly enriched in axonal guidance factors. In particular, the expression levels of SLIT3 and ROBO4, a protein–receptor pair,[41] were markedly increased. Immunofluorescence and qPCR experiments also confirmed the significant upregulation of SLIT3 and ROBO4 in TG-treated TKE2 cells in vitro and in mice corneal epithelium in vivo, suggesting that the SLIT3–ROBO4 pathway may be a downstream pathway of ER stress inhibiting corneal repair. Studies in various tissues have found a regulatory relationship between AGMs and ER stress; most of these studies reported the inhibitory effect of AGMs on ER stress, including molecules of the netrin, ephrin, and semaphorin families.[42–46] However, in the study of neurons, it was found that ER stress has a degradation effect on netrin-1.[47] To our knowledge, this study is the first report on ER stress regulating the SLIT family.

In the SLIT family, SLIT2 has been shown to promote diabetic corneal epithelial repair according to our group's

previous study[28] and inhibit corneal neovascularization.[48] However, the roles of SLIT1 and SLIT3 in the cornea have not been studied. SLIT3 is a protein secreted by the SLIT family of glycoproteins and is often considered a proangiogenic factor.[49,50] Several studies have confirmed that SLIT3 can regulate bone formation and regeneration by promoting angiogenesis.[51–54] Here, we found that the cornea as an avascular tissue has low expression of SLIT3; however, under ER stress, SLIT3 expression in the corneal epithelium was greatly increased. Exogenous SLIT3 supplementation significantly inhibited corneal epithelial wound healing, and, on the contrary, TG caused a delay of corneal wound healing that was reversed by inhibition of SLIT3. Given that corneal epithelial repair relies on the proliferation and migration of corneal epithelial cells, we conducted in vitro experiments to study the effect of SLIT3 on the proliferation and migration of mouse TKE2 cells. The results indicated that SLIT3 may suppress corneal re-epithelialization by inhibiting the proliferation and migration ability of corneal epithelial cells. In line with our findings, previous research showed that SLIT3 overexpression significantly reduces granulosa cell proliferation.[55] In terms of neural repair, recent studies have shown that SLIT3 plays a crucial role in controlling the formation of new neural bridges and proper axon regeneration after peripheral nerve transection injuries,[56] as well as in peripheral nerve repair after injury.[57] The cornea is the most densely innervated tissue of the body; after corneal injury, the regeneration of the local sensory nerves is regulated by numerous complex molecules.[19,20] Different AGMs have distinct effects on corneal nerve growth. For example, during early development, both Sema3A and SLIT2 are involved in preventing nerves from entering the corneal stroma. However, in the later stages of development, Sema3A continues to negatively regulate nerve entry into the corneal epithelium, whereas SLIT2 actively regulates nerve growth by increasing nerve branching within the corneal epithelium.[58] However, there are currently no reports on the effect of SLIT3 on corneal nerve innervation. The present study revealed that SLIT3 inhibits the regeneration of nerve fibers during corneal wound healing, indicating that it acts as a negative regulator for corneal nerve fiber regeneration. These findings suggest that ER stress may impair normal corneal regeneration by inducing SLIT3 overexpression.

SLIT3 primarily exerts its effects through binding to its receptors, which include ROBO1, ROBO2, ROBO3, and ROBO4.[41] Our RNA sequencing data and in vitro/vivo experimental validation demonstrate a significant upregulation of ROBO4 expression in corneal epithelial cells under ER stress. In multiple studies on angiogenesis, it has been reported that there is a SLIT3-ROBO4 pathway.[50,59–61] Studies in vascular endothelial cells have shown that ligand SLIT3 inhibits ROBO4 shedding to enhance ROBO4 signaling.[62] In the present study, we found that the increased expression of SLIT3 and ROBO4 induced by TG were significantly inhibited by SLIT3-specific siRNA, indicating that TG induced ER stress enhanced ROBO4 expression by SLIT3. However, the interaction mechanism between SLIT3 and ROBO4 in corneal epithelial cells still needs to be elucidated in future research. ROBO4-specific siRNA effectively restored ER stress and SLIT3 delayed corneal epithelial and nerve repair, suggesting that ER stress–induced SLIT3 overexpression may suppress the regeneration of corneal epithelium and nerves mainly through ROBO4 receptors. Zhang et al. found that ROBO4 deficiency accelerates skin wound healing.[63] Cai et al. showed that inhibition of ROBO4 expression promotes the proliferation and migration of human brain microvascular endothelial cells (HBMECs).[64] These studies indirectly support our conclusions. However, we have not yet identified the downstream mechanisms by which SLIT3–ROBO4 signaling affects corneal epithelial repair and nerve regeneration under ER stress.

In summary, our findings confirmed that ER stress inhibits corneal epithelial and nerve regeneration by activating the SLIT3–ROBO4 pathway. This study reveals a new mechanism by which ER stress regulates disease pathology and provides a new potential target for the treatment of corneal wound healing.

Acknowledgments

Support from the Natural Science Foundation of Shandong Province (ZR2022MH026 and ZR2020QH146), the National Natural Science Foundation of China (82371029 and 82000851), Qingdao Shinan District Science and Technology Plan Project (2022-2-018-YY), Youth Science Fund Cultivation Support Program Project of Shandong First Medical University (202201-121), the Innovation Project of Shandong Academy of Medical Sciences, the Academic promotion program of Shandong First Medical University (2019ZL001), and the Taishan Scholar Project of Shandong Province (tsqn20221163).

Author Contributions: R. Chen conducted experiments, collected and analyzed data, and wrote the manuscript. Y. Wang conducted experiments and collected data. Z. Zhang conducted some experiments and analyzed some data. X. Wang, Y. Li, M. Wang, H. Wang, and M. Dong analyzed the data. Q. Zhou guided the idea of the article. L. Yang designed the study, analyzed the data, and contributed to writing the manuscript.

Disclosure: **R. Chen**, None; **Y. Wang**, None; **Z. Zhang**, None; **X. Wang**, None; **Y. Li**, None; **M. Wang**, None; **H. Wang**, None; **M. Dong**, None; **Q. Zhou**, None; **L. Yang**, None

References

1. Belmonte C, Aracil A, Acosta MC, Luna C, Gallar J. Nerves and sensations from the eye surface. *Ocul Surf*. 2004;2:248–253.
2. Al-Aqaba MA, Dhillon VK, Mohammed I, Said DG, Dua HS. Corneal nerves in health and disease. *Prog Retin Eye Res*. 2019;73:100762.
3. Pakyurek H, Aykota MR, Kilic-Erkek O, Ozban M, Senol H, Bor-Kucukatay M. Investigation of time-dependent alterations in adipokine levels and endoplasmic reticulum stress markers in obese patients with laparoscopic sleeve gastrectomy. *Life Sci*. 2023;330:121987.
4. Berrak Rencüzoğullari Ö, Tornaci S, Çelik Y, et al. The protective impact of growth hormone against rotenone-induced apoptotic cell death via acting on endoplasmic reticulum stress and autophagy axis. *Turk J Biol*. 2023;47:29–43.
5. Straub IR, Weraarpachai W, Shoubridge EA. Multi-OMICS study of a CHCHD10 variant causing ALS demonstrates metabolic rewiring and activation of endoplasmic reticulum and mitochondrial unfolded protein responses. *Hum Mol Genet*. 2021;30:687–705.
6. Reddy SS, Prabhakar YK, Kumar CU, Reddy PY, Reddy GB. Effect of vitamin B(12) supplementation on retinal lesions in diabetic rats. *Mol Vis*. 2020;26:311–325.
7. Chen S, Chen J, Hua X, et al. The emerging role of XBP1 in cancer. *Biomed Pharmacother*. 2020;127:110069.
8. Nishitoh H. CHOP is a multifunctional transcription factor in the ER stress response. *J Biochem*. 2012;151:217–219.

9. Hong SC, Ha JH, Lee JK, Jung SH, Kim JC. In vivo anti-inflammation potential of Aster koraiensis extract for dry eye syndrome by the protection of ocular surface. *Nutrients*. 2020;12:3245.
10. Cho BJ, Hwang JS, Shin YJ, Kim JW, Chung TY, Hyon JY. Rapamycin rescues endoplasmic reticulum stress-induced dry eye syndrome in mice. *Invest Ophthalmol Vis Sci*. 2019;60:1254–1264.
11. Martinez-Carrasco R, Fini ME. Dynasore protects corneal epithelial cells subjected to hyperosmolar stress in an in vitro model of dry eye epitheliopathy. *Int J Mol Sci*. 2023;24:4735.
12. Ozge G, Karaca U, Savran M, et al. Salubrinal ameliorates inflammation and neovascularization via the caspase 3/enos signaling in an alkaline-induced rat corneal neovascularization model. *Medicina (Kaunas)*. 2023;59:323.
13. Huang Y, Lin L, Yang Y, et al. Effect of tauroursodeoxycholic acid on inflammation after ocular alkali burn. *Int J Mol Sci*. 2022;23:11717.
14. Wang X, Li W, Zhou Q, et al. MANF promotes diabetic corneal epithelial wound healing and nerve regeneration by attenuating hyperglycemia-induced endoplasmic reticulum stress. *Diabetes*. 2020;69:1264–1278.
15. Kruger RP, Aurandt J, Guan KL. Semaphorins command cells to move. *Nat Rev Mol Cell Biol*. 2005;6:789–800.
16. Hou ST, Jiang SX, Smith RA. Permissive and repulsive cues and signalling pathways of axonal outgrowth and regeneration. *Int Rev Cell Mol Biol*. 2008;267:125–181.
17. Dun XP, Parkinson DB. Role of netrin-1 signaling in nerve regeneration. *Int J Mol Sci*. 2017;18:491.
18. Schwend T, Lwigale PY, Conrad GW. Nerve repulsion by the lens and cornea during cornea innervation is dependent on Robo-Slit signaling and diminishes with neuron age. *Dev Biol*. 2012;363:115–127.
19. Zhou Q, Yang L, Wang Q, Li Y, Wei C, Xie L. Mechanistic investigations of diabetic ocular surface diseases. *Front Endocrinol (Lausanne)*. 2022;13:1079541.
20. Yu FX, Lee PSY, Yang L, et al. The impact of sensory neuropathy and inflammation on epithelial wound healing in diabetic corneas. *Prog Retin Eye Res*. 2022;89:101039.
21. Guaiquil VH, Xiao C, Lara D, Dimailig G, Zhou Q. Expression of axon guidance ligands and their receptors in the cornea and trigeminal ganglia and their recovery after corneal epithelium injury. *Exp Eye Res*. 2022;219:109054.
22. Lee PS, Gao N, Dike M, et al. Opposing effects of neuropilin-1 and -2 on sensory nerve regeneration in wounded corneas: role of Sema3C in ameliorating diabetic neurotrophic keratopathy. *Diabetes*. 2019;68:807–818.
23. Zhang Y, Chen P, Di G, Qi X, Zhou Q, Gao H. Netrin-1 promotes diabetic corneal wound healing through molecular mechanisms mediated via the adenosine 2B receptor. *Sci Rep*. 2018;8:5994.
24. Kaplan N, Fatima A, Peng H, Bryar PJ, Lavker RM, Getsios S. EphA2/Ephrin-A1 signaling complexes restrict corneal epithelial cell migration. *Invest Ophthalmol Vis Sci*. 2012;53:936–945.
25. Tong M, Jun T, Nie Y, Hao J, Fan D. The role of the Slit/Robo signaling pathway. *J Cancer*. 2019;10:2694–2705.
26. Basha S, Jin-Smith B, Sun C, Pi L. The SLIT/ROBO pathway in liver fibrosis and cancer. *Biomolecules*. 2023;13:785.
27. Iida C, Ohsawa S, Taniguchi K, Yamamoto M, Morata G, Igaki T. JNK-mediated Slit-Robo signaling facilitates epithelial wound repair by extruding dying cells. *Sci Rep*. 2019;9:19549.
28. Le T, Dewei L, Lixin X, Qingjun Z. Protective effects of Slit2 on corneal epithelium and nerves in diabetic mice and its mechanism. *J Exp Ophthalmol*. 2022;40:216–226.
29. Puri S, Moreno IY, Sun M, et al. Hyaluronan supports the limbal stem cell phenotype during ex vivo culture. *Stem Cell Res Ther*. 2022;13:384.
30. Cao Q, Peng D, Wang J, Reinach PS, Yan D. Unraveling the intricate network of lncRNAs in corneal epithelial wound healing: insights into the regulatory role of linc17500. *Transl Vis Sci Technol*. 2024;13:4.
31. Wan L, Bai X, Zhou Q, et al. The advanced glycation end-products (AGEs)/ROS/NLRP3 inflammasome axis contributes to delayed diabetic corneal wound healing and nerve regeneration. *Int J Biol Sci*. 2022;18:809–825.
32. Okada Y, Zhang Y, Zhang L, et al. Shp2-mediated MAPK pathway regulates ΔNp63 in epithelium to promote corneal innervation and homeostasis. *Lab Invest*. 2020;100:630–642.
33. Chen J, Chen P, Backman LJ, Zhou Q, Danielson P. Ciliary neurotrophic factor promotes the migration of corneal epithelial stem/progenitor cells by up-regulation of MMPs through the phosphorylation of Akt. *Sci Rep*. 2016;6:25870.
34. Chen J, Lan J, Liu D, et al. Ascorbic acid promotes the stemness of corneal epithelial stem/progenitor cells and accelerates epithelial wound healing in the cornea. *Stem Cells Transl Med*. 2017;6:1356–1365.
35. Subramanian A, Tamayo P, Mootha VK, et al. Gene set enrichment analysis: a knowledge-based approach for interpreting genome-wide expression profiles. *Proc Natl Acad Sci USA*. 2005;102:15545–15550.
36. Chen K, Li Y, Zhang X, Ullah R, Tong J, Shen Y. The role of the PI3K/AKT signalling pathway in the corneal epithelium: recent updates. *Cell Death Dis*. 2022;13:513.
37. Jackson TR, Patterson SI, Thastrup O, Hanley MR. A novel tumour promoter, thapsigargin, transiently increases cytoplasmic free Ca2+ without generation of inositol phosphates in NG115-401L neuronal cells. *Biochem J*. 1988;253:81–86.
38. Thastrup O, Cullen PJ, Drøbak BK, Hanley MR, Dawson AP. Thapsigargin, a tumor promoter, discharges intracellular Ca2+ stores by specific inhibition of the endoplasmic reticulum Ca2(+)-ATPase. *Proc Natl Acad Sci USA*. 1990;87:2466–2470.
39. Wang G, Xue Y, Wang Y, et al. The role of autophagy in the pathogenesis of exposure keratitis. *J Cell Mol Med*. 2019;23:4217–4228.
40. De Paiva CS, Pflugfelder SC, Li DQ. Cell size correlates with phenotype and proliferative capacity in human corneal epithelial cells. *Stem Cells*. 2006;24:368–375.
41. Blockus H, Chédotal A. Slit-Robo signaling. *Development*. 2016;143:3037–3044.
42. Choi SW, Oh H, Park SY, et al. Netrin-1 attenuates hepatic steatosis via UNC5b/PPARγ-mediated suppression of inflammation and ER stress. *Life Sci*. 2022;311:121149.
43. Zhong S, Pei D, Shi L, Cui Y, Hong Z. Ephrin-B2 inhibits Aβ(25-35)-induced apoptosis by alleviating endoplasmic reticulum stress and promoting autophagy in HT22 cells. *Neurosci Lett*. 2019;704:50–56.
44. Li M, Jin E, Zhu L, et al. Semaphorin 3A inhibits endoplasmic reticulum stress induced by high glucose in Müller cells. *Curr Eye Res*. 2023;48:70–79.
45. Zhang Y, Pusch S, Innes J, et al. Mutant IDH sensitizes gliomas to endoplasmic reticulum stress and triggers apoptosis via miR-183-mediated inhibition of semaphorin 3E. *Cancer Res*. 2019;79:4994–5007.
46. Tsuruma K, Nishimura Y, Kishi S, Shimazawa M, Tanaka T, Hara H. SEMA4A mutations lead to susceptibility to light irradiation, oxidative stress, and ER stress in retinal pigment epithelial cells. *Invest Ophthalmol Vis Sci*. 2012;53:6729–6737.

Investigative Ophthalmology & Visual Science

47. Binet F, Mawambo G, Sitaras N, et al. Neuronal ER stress impedes myeloid-cell-induced vascular regeneration through IRE1α degradation of netrin-1. *Cell Metab*. 2013;17:353–371.
48. Han X, Zhang MC. Potential anti-angiogenic role of Slit2 in corneal neovascularization. *Exp Eye Res*. 2010;90:742–749.
49. Wang S, Huang S, Johnson S, et al. Tissue-specific angiogenic and invasive properties of human neonatal thymus and bone MSCs: role of SLIT3-ROBO1. *Stem Cells Transl Med*. 2020;9:1102–1113.
50. Paul JD, Coulombe KLK, Toth PT, et al. SLIT3-ROBO4 activation promotes vascular network formation in human engineered tissue and angiogenesis in vivo. *J Mol Cell Cardiol*. 2013;64:124–131.
51. Li J, Wu G, Xu C, et al. Slit guidance ligand 3 (SLIT3) loaded in hydrogel microparticles enhances the tendon-bone healing through promotion of type-H vessel formation: an experimental study in mice. *Int J Mol Sci* 2023;24:13638.
52. Dadwal UC, Bhatti FUR, Awosanya OD, et al. The effects of bone morphogenetic protein 2 and thrombopoietin treatment on angiogenic properties of endothelial cells derived from the lung and bone marrow of young and aged, male and female mice. *FASEB J*. 2021;35:e21840.
53. Tian S, Zou Y, Wang J, Li Y, An BZ, Liu YQ. Protective effect of Du-Zhong-Wan against osteoporotic fracture by targeting the osteoblastogenesis and angiogenesis couple factor SLIT3. *J Ethnopharmacol*. 2022;295:115399.
54. Xu R, Yallowitz A, Qin A, et al. Targeting skeletal endothelium to ameliorate bone loss. *Nat Med*. 2018;24:823–833.
55. Xu R, Qin N, Xu X, Sun X, Chen X, Zhao J. Implication of SLIT3-ROBO1/ROBO2 in granulosa cell proliferation, differentiation and follicle selection in the prehierarchical follicles of hen ovary. *Cell Biol Int*. 2018;42:1643–1657.
56. Dun XP, Parkinson DB. Classic axon guidance molecules control correct nerve bridge tissue formation and precise axon regeneration. *Neural Regen Res*. 2020;15:6–9.
57. Chen B, Carr L, Dun XP. Dynamic expression of Slit1-3 and Robo1-2 in the mouse peripheral nervous system after injury. *Neural Regen Res*. 2020;15:948–958.
58. Kubilus JK, Linsenmayer TF. Developmental guidance of embryonic corneal innervation: roles of Semaphorin3A and Slit2. *Dev Biol*. 2010;344:172–184.
59. Zhang B, Xiao W, Qiu H, et al. Heparan sulfate deficiency disrupts developmental angiogenesis and causes congenital diaphragmatic hernia. *J Clin Invest*. 2014;124:209–221.
60. Dou C, Wang H, Zhou G, Zhu H, Wen H, Xu S. Slit3 regulates migration of endothelial progenitor cells by activation of the RhoA/Rho kinase pathway. *Int J Clin Exp Pathol*. 2018;11:3398–3404.
61. Chen K, Fan Y, Gu J, et al. In vivo screening of natural products against angiogenesis and mechanisms of anti-angiogenic activity of Deoxysappanone B 7,4′-dimethyl ether. *Drug Des Devel Ther*. 2020;14:3069–3078.
62. Xiao W, Pinilla-Baquero A, Faulkner J, et al. Robo4 is constitutively shed by ADAMs from endothelial cells and the shed Robo4 functions to inhibit Slit3-induced angiogenesis. *Sci Rep*. 2022;12:4352.
63. Zhang F, Prahst C, Mathivet T, et al. The Robo4 cytoplasmic domain is dispensable for vascular permeability and neovascularization. *Nat Commun*. 2016;7:13517.
64. Cai H, Xue Y, Li Z, et al. Roundabout4 suppresses glioma-induced endothelial cell proliferation, migration and tube formation in vitro by inhibiting VEGR2-mediated PI3K/AKT and FAK signaling pathways. *Cell Physiol Biochem*. 2015;35:1689–1705.

Investigative Ophthalmology & Visual Science